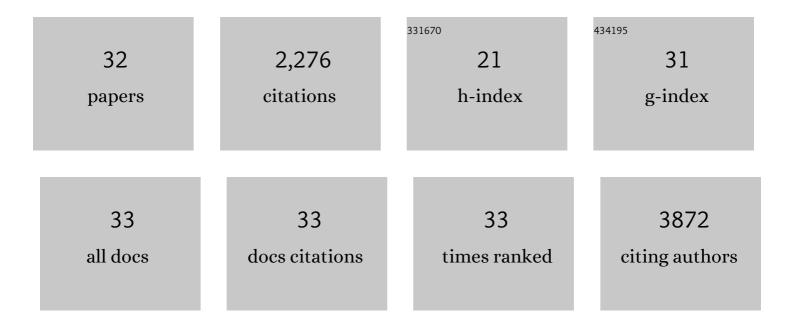
## Molly Meng-Jung Li

List of Publications by Year in descending order

Source: https://exaly.com/author-pdf/1051966/publications.pdf Version: 2024-02-01



#	Article	IF	CITATIONS
1	MoS2 monolayer catalyst doped with isolated Co atoms for the hydrodeoxygenation reaction. Nature Chemistry, 2017, 9, 810-816.	13.6	683
2	Interstitial modification of palladium nanoparticles with boron atoms as a green catalyst for selective hydrogenation. Nature Communications, 2014, 5, 5787.	12.8	196
3	Enhanced CO2 hydrogenation to methanol over CuZn nanoalloy in Ga modified Cu/ZnO catalysts. Journal of Catalysis, 2016, 343, 157-167.	6.2	152
4	Structural Studies of Bulk to Nanosize Niobium Oxides with Correlation to Their Acidity. Journal of the American Chemical Society, 2017, 139, 12670-12680.	13.7	125
5	CO <sub>2</sub> Hydrogenation to Methanol over Catalysts Derived from Single Cationic Layer CuZnGa LDH Precursors. ACS Catalysis, 2018, 8, 4390-4401.	11.2	121
6	Transition metal-doped nickel phosphide nanoparticles as electro- and photocatalysts for hydrogen generation reactions. Applied Catalysis B: Environmental, 2019, 242, 186-193.	20.2	120
7	Bimetallic catalysts for green methanol production <i>via</i> CO <sub>2</sub> and renewable hydrogen: a mini-review and prospects. Catalysis Science and Technology, 2018, 8, 3450-3464.	4.1	104
8	A promising low pressure methanol synthesis route from CO <sub>2</sub> hydrogenation over Pd@Zn core–shell catalysts. Green Chemistry, 2017, 19, 270-280.	9.0	82
9	Tailored transition metal-doped nickel phosphide nanoparticles for the electrochemical oxygen evolution reaction (OER). Chemical Communications, 2018, 54, 8630-8633.	4.1	73
10	The role of acid and metal sites in hydrodeoxygenation of guaiacol over Ni/Beta catalysts. Catalysis Science and Technology, 2020, 10, 810-825.	4.1	69
11	Methanol Synthesis at a Wide Range of H <sub>2</sub> /CO <sub>2</sub> Ratios over a Rhâ€In Bimetallic Catalyst. Angewandte Chemie - International Edition, 2020, 59, 16039-16046.	13.8	54
12	Enhanced chemoselective hydrogenation of dimethyl oxalate to methyl glycolate over bimetallic Ag–Ni/SBA-15 catalysts. Applied Catalysis A: General, 2015, 505, 344-353.	4.3	47
13	Energy Decarbonization via Green H <sub>2</sub> or NH <sub>3</sub> ?. ACS Energy Letters, 2022, 7, 1021-1033.	17.4	45
14	The remarkable activity and stability of a dye-sensitized single molecular layer MoS <sub>2</sub> ensemble for photocatalytic hydrogen production. Chemical Communications, 2015, 51, 13496-13499.	4.1	43
15	Cooperative catalysis for the direct hydrodeoxygenation of vegetable oils into diesel-range alkanes over Pd/NbOPO <sub>4</sub> . Chemical Communications, 2016, 52, 5160-5163.	4.1	43
16	Surfactant-free nickel–silver core@shell nanoparticles in mesoporous SBA-15 for chemoselective hydrogenation of dimethyl oxalate. Chemical Communications, 2016, 52, 2569-2572.	4.1	39
17	Morphology, Chemical Composition and Phase Transformation of Hydrothermal Derived Sodium Titanate. Journal of the American Ceramic Society, 2012, 95, 3297-3304.	3.8	34
18	Graphitic carbon nitride catalysed photoacetalization of aldehydes/ketones under ambient conditions. Chemical Communications, 2016, 52, 2772-2775.	4.1	34

MOLLY MENG-JUNG LI

#	Article	IF	CITATIONS
19	Lithium and boron as interstitial palladium dopants for catalytic partial hydrogenation of acetylene. Chemical Communications, 2017, 53, 601-604.	4.1	31
20	Shape selectivity of zeolite catalysts for the hydrodeoxygenation of biocrude oil and its model compounds. Microporous and Mesoporous Materials, 2020, 309, 110561.	4.4	30
21	Enhanced propylene oxide selectivity for gas phase direct propylene epoxidation by lattice expansion of silver atoms on nickel nanoparticles. Applied Catalysis B: Environmental, 2019, 243, 304-312.	20.2	26
22	Structure–Activity Correlations for BrÃ,nsted Acid, Lewis Acid, and Photocatalyzed Reactions of Exfoliated Crystalline Niobium Oxides. ChemCatChem, 2017, 9, 144-154.	3.7	22
23	Importance of the structural integrity of a carbon conjugated mediator for photocatalytic hydrogen generation from water over a CdS–carbon nanotube–MoS <sub>2</sub> composite. Chemical Communications, 2016, 52, 13596-13599.	4.1	20
24	Pd@Zn core–shell nanoparticles of controllable shell thickness for catalytic methanol production. Catalysis Science and Technology, 2016, 6, 7698-7702.	4.1	19
25	The remarkable activity and stability of a highly dispersive beta-brass Cu-Zn catalyst for the production of ethylene glycol. Scientific Reports, 2016, 6, 20527.	3.3	18
26	Methanol Synthesis at a Wide Range of H <sub>2</sub> /CO <sub>2</sub> Ratios over a Rhâ€In Bimetallic Catalyst. Angewandte Chemie, 2020, 132, 16173-16180.	2.0	17
27	Influence of ionic mobility on the phase transformation route in Y3Al5O12 (YAG) stoichiometry. Journal of the European Ceramic Society, 2011, 31, 2099-2106.	5.7	14
28	Evaluation of BrÃ,nsted and Lewis acid sites in H-ZSM-5 and H-USY with or without metal modification using probe molecule-synchrotron X-ray powder diffraction. Applied Catalysis A: General, 2020, 596, 117528.	4.3	5
29	Evaluation of the molecular poisoning phenomenon of W sites in ZSM-5 <i>via</i> synchrotron X-ray powder diffraction. Chemical Communications, 2018, 54, 7014-7017.	4.1	3
30	Crafting an active center with a local charge density gradient to facilitate photocatalytic ethylene production from CO2. Current Opinion in Green and Sustainable Chemistry, 2022, 36, 100646.	5.9	3
31	Thermal Alteration in Adsorption Sites over SAPO $\hat{a} \in 3$ 4 Zeolite. Angewandte Chemie, 0, , .	2.0	1
32	Understanding catalysis for processing glycerol and glycerol-based derivatives for the production of value added chemicals. Catalysis, 2019, , 267-296.	1.0	0

3